A Letters Journal Exploring the Frontiers of Physics

March 2009

EPL, **85** (2009) 57008
doi: 10.1209/0295-5075/85/57008

www.epljournal.org

Waiting time distributions of electron transfers through quantum dot Aharonov-Bohm interferometers

S. Welack[1(a)], S. Mukamel[2] and YiJing Yan[1(b)]

[1] *Department of Chemistry, Hong Kong University of Science and Technology - Kowloon, Hong Kong*
[2] *Department of Chemistry, University of California - Irvine, CA, USA*

received 6 November 2008; accepted in final form 13 February 2009
published online 19 March 2009

PACS 73.63.Kv – Quantum dots
PACS 74.40.+k – Fluctuations (noise, chaos, nonequilibrium superconductivity, localization, etc.)
PACS 73.23.Hk – Coulomb blockade; single-electron tunneling

Abstract – We present an analysis of waiting time distributions of consecutive single-electron transfers through a double-quantum-dot Aharonov-Bohm interferometer. Waiting time distributions qualitatively indicate the presence of interferences and provide information on orbital-detuning and coherent interdot-electron transfer. The frequencies of interdot-transfer–induced oscillations are Aharonov-Bohm phase sensitive, while those due to level detuning are phase independent. The signature of the quantum interference in the waiting-time distribution is more apparent for weakly coupled electron transfer detectors.

Introduction. – Double-quantum-dot (DQD) junctions provide an experimental setup to study phase coherent transport [1–3] and to realize Aharonov-Bohm (AB) interferometers [4–6]. So far theoretical studies on transport properties of DQD-AB interferometers have been focused on average current [7–14] and shot noise [15–18] properties. Recently time-resolved detection of single-electron transfers in single QD [19–22] and DQD in series has become experimentally feasible [23]. The waiting-time distribution (WTD) of consecutive electron transfers can be obtained from time series analysis and provide detailed information on QDs [24,25] and single molecules [26]. They were found to be sensitive to interference due to multiple-electron paths in DQD junctions [24] and contain more detailed information than current and noise measurements [25].

In this work we present a WTD analysis of single-electron transfer through a model DQD-AB interferometer. The WTD signal reveals the energetic structure, Coulomb interaction, and quantum interference of the DQD. These quantities are connected with qualitatively distinguishable oscillations in the WTD. The frequencies of these oscillations are sensitive to the AB phase, $\phi \equiv 2\pi\Phi/\Phi_0$, and are suppressed at $\phi = 2n\pi$ for an integer n when interdot transfer is present. Here, Φ is the magnetic flux perpendicular to the junction and $\Phi_0 = h/e$ the magnetic flux quanta. In contrast, the frequencies of the oscillations purely due to energy detunings of the DQD orbitals are ϕ-independent. We show that their detection requires weakly coupled electron detectors thereby avoiding to inflict fast decoherence on the DQD. To this end, we exploit a master equation in the many-body Fock space of the DQD, assuming weak system-reservoir coupling.

The applied magnetic flux can be detected by current measurements and the shot noise Fano factor is quantitatively shifted by interdot transfers [16,17]. For WTD, a qualitatively distinct dependence on interdot-electron transfers and orbital detunings is given by the oscillations. The information content obtained through WDT is can be mostly replicated by the full shot noise spectrum [25] and analysis of WTD can serve as an alternative approach to study the system under investigation.

The paper is organized as follows. In the second section we present the Hamiltonian of the AB-DQD interferometer. In the third section, we derive the quantum master equation and the expressions for the WTD. The fourth section is dedicated the discussion of the analytical and numerical results, followed by conclusion and outlook.

Hamiltonian. – The set-up under consideration is illustrated in fig. 1. We consider spinless electrons and each QD can hold only one electron at most. We decompose the total Hamiltonian of the DQD-AB interferometer junction

(a) E-mail: wesv@ust.hk
(b) E-mail: yyan@ust.hk

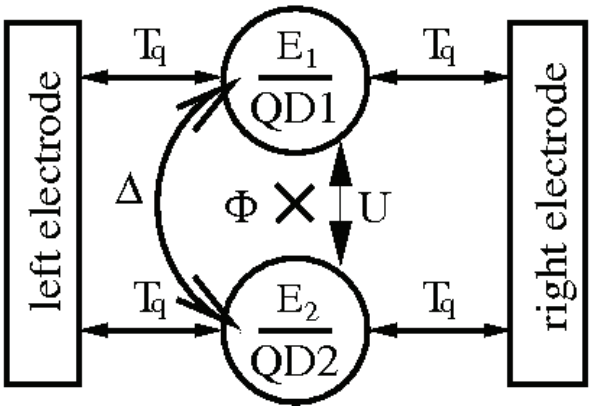

Fig. 1: Sketch of the DQD-AB interferometer and the involved parameters.

into $\tilde{H}_T = \tilde{H}_S + \tilde{H}_R + \tilde{H}_{SR}(\phi)$. The DQD part (system) reads

$$\tilde{H}_S = \sum_{s=1,2} \epsilon_s c_s^\dagger c_s + U c_1^\dagger c_1 c_2^\dagger c_2 - \Delta(c_1^\dagger c_2 + c_2^\dagger c_1). \quad (1)$$

Here, ϵ_s with $s=1$ or 2 is the orbital energy of the specified QD; U denotes the strength of the Coulomb repulsion between electrons; Δ is the interdot-electron transfer parameter in the DQD-AB interferometer. Measuring the electrons directly inside the DQD-AB interferometer would induce dephasing since acquisition of the transfer path information suppresses interference in accordance with the quantum-mechanical complementary principle [27] and the direct detection process can alterate the statistics [22]. The analysis of the WTB does not require the path information of transfers through the DQD-AB interferometer but only the counting of electrons entering and leaving the junction regardless of their path. We consider the electrodes as two independent free-electron reservoirs, $H_R = \sum_{\nu=l,r} \sum_q \epsilon_{q\nu} c_{q\nu}^\dagger c_{q\nu}$, which serve as weakly coupled electron transfer detectors and no additional apparatus for electron transfer measurement is applied to the system. The index ν denotes the left (l) or right (r) electrode, q their intrinsic degrees of freedom. The electron creation (annihilation) operators $c_s^\dagger$ and $c_{q\nu}^\dagger$ (c_s and $c_{q\nu}$) satisfy the anticommutator relations: $\{c_k, c_{k'}^\dagger\} = \delta_{kk'}$ and $\{c_k^\dagger, c_{k'}^\dagger\} = \{c_k, c_{k'}\} = 0$, for all $k, k' = s, q\nu$. The system-reservoirs coupling responsible for electron transfer between the electrodes and the DQD reads

$$\tilde{H}_{SR}(\phi) = \sum_{\nu=l,r} \sum_{sq} \left[T_{qs}^{(\nu)}(\phi) c_s^\dagger c_{q\nu} + \text{H.c.} \right]. \quad (2)$$

The AB phase ϕ-dependent transfer parameters satisfy $T_{q1}^{(\nu)}(\phi) = T_{q1} e^{i\phi_\nu/4}$ and $T_{q2}^{(\nu)}(\phi) = T_{q2} e^{-i\phi_\nu/4}$, for the two parallel dots pierced by the single magnetic flux considered here. The phase components ϕ_ν in the couplings elements $T_{q1,2}^{(\nu)}(\phi)$ satisfy $\phi_l = -\phi_r = \phi$. This relation accounts for the mirrored orientation of the couplings elements $T_{q1,2}^{(\nu)}(\phi)$ to the right electrode with respect to the left electrode. Hamiltonian (2) and the left/right phase relation were employed in previous theoretical studies [14–17].

Formalism. – We describe the DQD by the reduced density operator $\rho(t)$ of the system. Note that the interdot-electron transfer Δ in eq. (1) leads to off-diagonal elements in the system Hamiltonian $\tilde{H}_S$ in the orbital basis. We transform it into eigenbasis, $H_S = O^{-1}\tilde{H}_S O$, where O consists of the eigenvectors of $\tilde{H}_S$. The same transformation is applied to the creation and annihilation operators $\Psi_s = O^{-1} c_s O$ and $\Psi_s^\dagger = O^{-1} c_s^\dagger O$, with $s=1,2$ denoting the two orbitals of the DQD, such that $H_{SR} = O^{-1}\tilde{H}_{SR}O$. The standard perturbation theory leads to the quantum master equation in eigenbasis [24]:

$$\dot{\rho}(t) = -i\mathcal{L}\rho(t) + \sum_{\nu=l,r} (-\Pi_\nu + \Sigma_\nu^+ + \Sigma_\nu^-)\rho(t). \quad (3)$$

The system Liouvillian $\mathcal{L}\cdot = [H_S, \cdot\,]$ in eigenbasis describes the coherent dynamics. The dissipative superoperator in eq. (3) is separated into the diagonal contribution Π_ν that leaves the number of electrons in the system unchanged, and the off–diagonal Σ_ν^+ and Σ_ν^- for the increase and decrease the number of electrons in the DQD, respectively; see ref. [24] for the derivation. This separation is necessary in order to keep track of the trajectories of single-electron transfers.

Consider, for example, the scenario of detecting an electron entering the DQD through the left electrode at time t_0 and leaving through the right electrode at time t. The waiting-time distribution of consecutive electron transfer events is then given by the joint probability [24]

$$P_{l\to r}(t, t_0) = \text{tr}_S\{\Sigma_r^- S_{t,t_0} \Sigma_l^+ \rho_S(t_0)\}, \quad (4)$$

with $S_{t,t_0} = \exp[(-i\mathcal{L} - \Pi_l - \Pi_r)(t-t_0)]$ being the propagator of the system in the absence of transfer events at the electrodes within the waiting-time interval. Quantity (4) can be obtained from the time series of single directionally resolved electron transfers between the electrodes and the system. One has to record a sufficiently large number of the $l \to r$ events and generate a histogram of the number of occurrences as function of the time interval $t - t_0$. The histogram has to be normalized by the total number of considered events.

The aforementioned physically distinct dissipative components are formally given as [24] $\Sigma_\nu^+ = \sum_s \vec{\Psi}_s^\dagger \overleftarrow{\Psi}_{\nu s}^{(-)} + \overleftarrow{\Psi}_s \vec{\Psi}_{\nu s}^{\dagger(-)}$, $\Sigma_\nu^- = \sum_s \overleftarrow{\Psi}_s^\dagger \vec{\Psi}_{\nu s}^{(+)} + \vec{\Psi}_s \overleftarrow{\Psi}_{\nu s}^{\dagger(+)}$, and $\Pi_\nu = \sum_s \big(\vec{\Psi}_s^\dagger \vec{\Psi}_{\nu s}^{(+)} + \overleftarrow{\Psi}_s^\dagger \overleftarrow{\Psi}_{\nu s}^{(-)} + \text{H.c.} \big)$. The involved superoperators are defined as the left or right actions ($\vec{\Psi}\cdot \equiv \Psi\cdot$ or $\overleftarrow{\Psi}\cdot \equiv \cdot\Psi$) of the associated Hilbert-space Ψ-operators. Besides the annihilation (creation) operators Ψ_s ($\Psi_s^\dagger$) we also have to consider their auxiliaries [24,28]:

$$\Psi_{\nu s}^{(\pm)}(t, \phi) = \sum_{s'} \int_{t_0}^t \mathrm{d}t' C_{\nu s s'}^{(\pm)}(t - t'; \phi) e^{-i\mathcal{L}(t-t')} \Psi_{s'}. \quad (5)$$

Here, $C^{(+)}_{\nu ss'}(t;\phi)=\sum_{qq'}T^{(\nu)*}_{qs}(\phi)T^{(\nu)}_{q's'}(\phi)\langle c^\dagger_{q\nu}(t)c_{q'\nu}(0)\rangle_R$ and $C^{(-)}_{\nu ss'}(t;\phi)=\sum_{qq'}T^{(\nu)}_{qs}(\phi)T^{(\nu)*}_{q's'}(\phi)\langle c_{q\nu}(t)c^\dagger_{q'\nu}(0)\rangle_R$ are the AB phase-dependent interacting reservoir correlation functions. The trace over the reservoir degrees of freedom is denoted by $\langle\ldots\rangle_R$. Applying the given phase relations in $T^{(\nu)}_{qs}(\phi)$ and assuming further $T_{q1}=T_{q2}=T_q$ for the AB phase-free parts lead to the relations: $C^{(\pm)}_{\nu 11}(t)=C^{(\pm)}_{\nu 22}(t)=C^{(\pm)}_\nu(t)$, $C^{(\pm)}_{\nu 12}(t)=C^{(\pm)}_\nu(t)e^{i\phi_\nu/2}$, and $C^{(\pm)}_{\nu 21}(t)=C^{(\pm)}_\nu(t)e^{-i\phi_\nu/2}$. The auxiliary operators in their non-Markovian form (eq. (5)) can be numerically evaluated without further approximations as shown in refs. [24] and [28]. To derive analytical results we apply the Born-Markov approximation, together with the wide-band limit for the reservoir spectral density $\Gamma\equiv|T_q|^2\delta(\epsilon-\epsilon_{q\nu})$. The latter leads to $C^{(\pm)}_\nu(t)=\Gamma\int_0^\infty \mathrm{d}\epsilon\, f^{(\pm)}_\nu(\epsilon)e^{\mp i\epsilon t}$. Here, $f^+_\nu(\epsilon)=1-f^-_\nu(\epsilon)=[e^{(\beta(\epsilon-\mu_\nu)}+1]^{-1}\equiv f(\epsilon-\mu_\nu)$ is the Fermi distribution function, with β being the inverse temperature and μ_ν the Fermi energy of the electrode ν. The Born-Markov approximation amounts to replacing the range of time integration in eq. (5) with $(-\infty,\infty)$. As results, the auxiliary annihilation operators defined in eq. (5) can be evaluated as

$$\Psi^{(\pm)}_{\nu 1}=\Gamma f^\pm_\nu(\mathcal{L})(\Psi_1+\Psi_2 e^{\pm i\phi_\nu/2}), \tag{6a}$$

$$\Psi^{(\pm)}_{\nu 2}=\Gamma f^\pm_\nu(\mathcal{L})(\Psi_1 e^{\mp i\phi_\nu/2}+\Psi_2), \tag{6b}$$

which depend on the AB-phase but no longer on the time. The auxiliary creation operators $\Psi^{\dagger(\pm)}_{\nu s}$ are of similar expressions, but with the replacements of $\mathcal{L}\to-\mathcal{L}$, $\phi\to-\phi$ and $\Psi_s\to\Psi^\dagger_s$ in eq. (6). Note that since H_S is diagonal in the many-body Fock space, the action of the superoperator $f^\pm_\nu(\mathcal{L})$, which is determined by the Fermi function and the diagonal system Liouvillian, can be carried out easily. All the 16 auxiliary operators, $\Psi^{(\pm)}_{\nu s}$ and $\Psi^{\dagger(\pm)}_{\nu s}$ with $\nu=l,r$ and $s=1,2$, can now be evaluated (cf. eq. (6)) in terms of 4×4 matrices in the Fock-space representation. Consequently, the action of each dissipative tensor in the second term of eq. (3), which has been given in terms of the left and right multiplications of some Ψ_s ($\Psi^\dagger_s$) and $\Psi^{(\pm)}_{\nu s}$ ($\Psi^{\dagger(\pm)}_{\nu s}$) is now determined. It is worth to mention here that the approximation scheme explored in eq. (6) leads to an eq. (3) in Lindblad form.

Results. – We use the following parameter scheme to describe our calculation results. A bias of $2V$ is applied symmetrically $\mu_{l/r}=\mu_{\rm eq}\pm V$. Some theoretical investigation employed degenerated orbitals [16–18] for simplification while interesting effects could be predicted in the non-degenerate scenario [12–14,24] that had also been studied in experiment [4]. We consider the latter. The orbital energies of the DQD are set to be $\epsilon_1=\epsilon_g+\alpha$ and $\epsilon_2=\epsilon_g-\alpha$; *i.e.*, the orbital energy split (or detuning) is 2α. We set the vacuum DQD state $\epsilon_0=0$ as the energy zero, and $\epsilon_g=1$ the internal energy unit. In all calculations, $\mu_{\rm eq}=1.0$ and $T=0.1$.

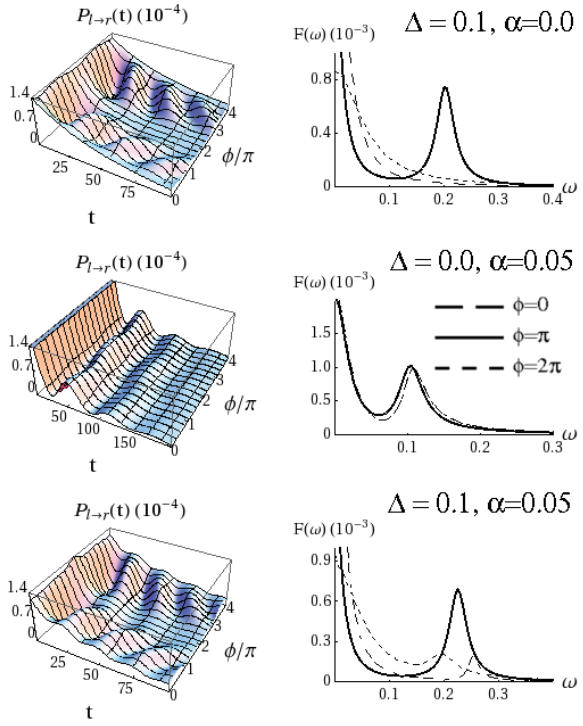

Fig. 2: $P_{l\to r}(t)$ (left panels) as functions of AB-phase ϕ and time t. The corresponding Fourier transformation $F(\omega)$ (right panels) at $\phi=0$ (dash), $\pi/2$ (solid), and π (dot), respectively. The upper, middle and bottom panels are for three representing sets of interdot transfer rate Δ and orbital detuning α. Other parameters are $U=1.0, T=0.1, 2V=0.2$ and $\mu_{eg}=1.0$ (in unit of ϵ_g); see text for details.

Figure 2 demonstrates the dependence of the waiting-time distributions $P_{l\to r}(t)$ (left panels) on the AB-phase ϕ, together with their Fourier transforms $F(\omega)$ (right panels) exemplified at three representing values of $\phi=0,\pi$, and 2π. The Coulomb repulsion parameter $U=1.0$ and the bias $2V=0.2$ are common, while the interdot transfer and orbital energy split parameters are $(\Delta,\alpha)=(0.1,0)$ in the upper, (0, 0.05) in the middle, and (0.1, 0.05) in the bottom panels, respectively. Clearly, the influences of Δ and α on the waiting-time distribution are qualitatively distinct, especially in the two limiting regimes. While $P_{l\to r}(t)$ shows only little dependence on ϕ in the dot orbital split case (the middle panel: $\Delta=0$ but $\alpha\neq0$), it is strikingly sensitive to the AB-phase in the interdot transfer case (the upper panel: $\Delta\neq0$ but $\alpha=0$). In the latter case, the characteristic oscillation is maximized at $\phi=\pi$, but disappears at $\phi=0$ and $\phi=2\pi$. These observations can be largely understood as follows.

The dot orbital split ($\Delta=0$ but $\alpha\neq0$) case resembles the transport through double slits. The resulting interference [24] persists and is sensitive to the AB-phase with a period of 2π as it was predicted for the electric current [13–17]. Here the decrease and increase of the amplitude of the WDT reflects this dependence of the current on the AB-phase, since it can be obtained from

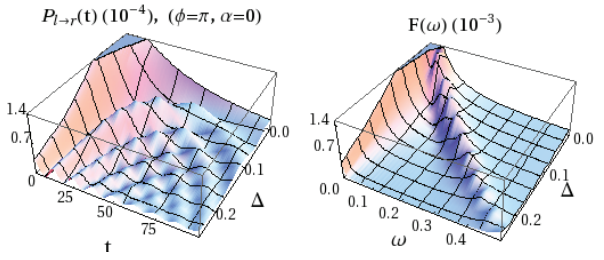

Fig. 3: $P_{l\to r}(t)$ as a function of interdot transfer rate Δ and the time t and the corresponding Fourier transformation $F(\omega)$. The AB-phase is $\phi=\pi$ and the orbital detuning $\alpha=0$. Other parameters are same as fig. 2.

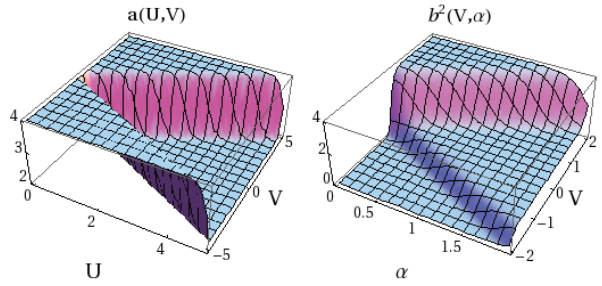

Fig. 4: The damping parameter $a(U,V)$ and the pre-exponential amplitude parameter $b^2(V,\alpha)$, as their functionial dependence, for the oscillation term $P_{osc}(t)$ (eq. (7)). Interdot-electron transfer is absent, $\Delta=0$.

WDT by integration [24]. This accounts for the basic feature observed in the middle panels of fig. 2.

In interdot transfer case (upper panels: $\Delta\neq 0$ but $\alpha=0$), the aforementioned double-slit feature is destroyed. The interdot transfer allows electrons to switch between the two pathways provided by the DQD. Thus, different phases can be accumulated as the electron transfer through the coupled DQD and the phase symmetry is broken along some of the possible transfer trajectories. As a result, the total accumulated phase depends on the value of ϕ with a period of 4π. This periodic behavior was recently predicted in ref. [17] for specific settings of the eigenenergies of the DQD-AB interferometer.

Here, it leads to a pure exponential decay of $P_{l\to r}(t)$ at the AB-phase $\phi=0$ or 2π. However, at other values of ϕ, it leads to an effective phase difference between the eigenlevels which are subject to an induced energy gap of 2Δ, responsible for the AB-phase activated oscillations observed in the upper panels of fig. 2.

In the intermediate regime shown in the bottom panels of fig. 2, oscillations can be observed for all ϕ; however, the Fourier transform reveals a frequency shift when the AB-phase is tuned by the magnetic field. At $\phi=\pi$, the observed frequency corresponds to the DQD eigenenergy gap ($2\sqrt{\Delta^2+\alpha^2}=0.224$), while at $\phi=0$ or 2π, it is blue or red shifted, respectively. The amplification of the oscillation at $\phi=\pi$ is characteristic for interdot transfer and allows to distinguish it from orbital detuning. The latter causes only small oscillations at $\phi=0$ or 2π.

Figure 3 examines further the influence of Δ on $P_{l\to r}(t)$ (left) and its spectrum $F(\omega)$ (right), with $\alpha=0$ and $\phi=\pi$, where oscillations due to AB-phase–activated interferences between the eigenlevels are at maximum. Note that the interference would remain dark at $\phi=0$ in this case; as can be seen the upper panels of fig. 2. The amplitude of $P_{l\to r}(t)$ oscillation decreases with Δ, which corresponds to a decreased average current through the DQD.

To analyze other coherent operation conditions, let us focus on the orbital-detuning ($\Delta=0$ and $\alpha\neq 0$) case where $\tilde{H}_S$ is diagonal. We also neglect the Liouville-space off-diagonal elements in $\Pi_l+\Pi_r$, which have a relatively small influence in the weak-coupling regime. As results, the propagator S_{t,t_0} in determining $P_{l\to r}(t,t_0)$ (eq. (4)) becomes diagonal, and the analytical solution is achievable. Moreover, the waiting-time distribution is separable into $P_{l\to r}(t)=P_{osc}(t)+P_{decay}(t)$.

The decaying terms $P_{decay}(t)$ depend only weakly on the AB-phase which would make it difficult to extract information. For the case of incoherent transport through single benzene molecules a detailed discussion of $P_{decay}(t)$ is provided in ref. [26] which can be applied to QD-systems as well.

As the coherent operation conditions are concerned, we focus only on the oscillation term, which is independent of the AB-phase for the orbital split case (cf. the middle panels of fig. 2).

$$P_{osc}(t)=p_0\Gamma^2 b^2(V,\alpha)e^{-2a(U,V)\Gamma t}\cos(2\alpha t), \qquad (7)$$

where p_0 is the initial vacuum state occupation number, $a(U,V)=a(U,-V)=f(U+V)+f(U-V)+2$, and

$$b(V,\alpha)=\frac{1+e^{2\alpha\beta}+2e^{(V+\alpha)\beta}}{e^{\beta(V+2\alpha+1)/2}}f(V+\alpha)f(V-\alpha). \qquad (8)$$

The left panel of fig. 4 depicts the damping parameter a as a function of U and V. It assumes the maximum value of 4 for small Coulomb coupling $U<V$ and is independent of α. Also the decay rate proportional to the system-electrode coupling strength Γ. Thus a weak coupling is required for the observability of interferences. This qualifies statistical analysis of waiting-time distributions as an indirect method to study internal processes indirectly avoiding fast decoherence in the system.

The right panel of fig. 4 depicts the pre-exponent parameter b^2 as function of V and α. It reveals further the parameter regimes where oscillations are observable. One condition is that $V<\alpha$. Oscillations are suppressed at negative bias larger than the DQD energy gap. The amplitude is strongly increased when $V>\alpha$. However, in this regime the decay rate $2a\Gamma$ may reach its maximum and prevent the observability of interferences. Apparently, the presence of strong Coulomb coupling, as well as operating at small bias regime, are favored for the observation of interference effects by means of waiting-time distributions.

Conclusion. – In conclusion, a Markovian quantum master equation in the Fock space was formulated and employed to calculate the waiting-time distribution of consecutive electron transfers in AB interferometers.

Based on this we describe a novel statistical method to determine quantum interferences, interdot-electron transfers, orbital detuning and the AB-phase. Orbital detuning and interdot transfer induce oscillations in the waiting-time distribution in the presence of interference. The two cases can be distinguished qualitatively since the frequency of the latter one is sensitive to the AB-phase. The observability of oscillations, from which the aforementioned parameters can be quantitatively deduced, requires the presence of strong Coulomb interaction, small bias and a weak electrode-system coupling.

The predicted effects can be tested by combining QD-AB experiments [3] with recent single-electron counting experiments [23]. The DQD may have to be employed in parallel geometry. Such an experiment would allow to extend single-electron counting spectroscopy [25,26] to AB-interferometers, and thus, provide more detailed information than conventional current and noise measurements.

The indirectness of the statistical detection avoids fast decoherence but a large number of transfer events is necessary in order to extract information. Also other sources of decoherence like coupling to phonon bath have to be minimized. The signature of interferences in the waiting-time distribution can survive in the presence of a phonon bath [25].

* * *

Support from the RGC (604007 and 604508) of Hong Kong (to YJY), NSF (CHE-0745892/CBC-0533162) and NIRT (EEC 0303389) of USA (to SM) is acknowledged.

REFERENCES

[1] Waugh F. R. *et al.*, *Phys. Rev. Lett.*, **75** (1995) 705.
[2] Chen J. C., Chang A. M. and Melloch M. R., *Phys. Rev. Lett.*, **92** (2004) 176801.
[3] Holleitner A. W., Blick R. H., Hüttel A. K., Eberl K. and Kotthaus J. P., *Science*, **297** (2002) 70.
[4] Holleitner A. W., Decker C. R., Qin H., Eberl K. and Blick R. H., *Phys. Rev. Lett.*, **87** (2001) 256802.
[5] Ihn T., Sigrist M., Ensslin K., Wegscheider W. and Reinwald M., *New J. Phys.*, **9** (2007) 111.
[6] Sigrist M., Ihn T., Ensslin K., Loss D., Reinwald M. and Wegscheider W., *Phys. Rev. Lett.*, **96** (2006) 036804.
[7] Apel V. M., Davidovich M. A., Chiappe G. and Anda E. V., *Phys. Rev. B*, **72** (2005) 125302.
[8] Moldoveanu V., Tolea M., Aldea A. and Tanatar B., *Phys. Rev. B*, **71** (2005) 125338.
[9] Mourokh L. G. and Smirnov A. Y., *Phys. Rev. B*, **72** (2005) 033310.
[10] Simon P. and Feinberg D., *Phys. Rev. Lett.*, **97** (2006) 247207.
[11] Kang K. and Cho S. Y., *J. Phys.: Condens. Matter*, **16** (2004) 117.
[12] Kubala B. and König J., *Phys. Rev. B*, **65** (2002) 245301.
[13] Li F., Li X.-Q., Zhang W.-M. and Gurvitz S. A., *Magnetic field switching in parallel quantum dots,* arXiv:0803.1618.
[14] Tokura Y., Nakano H. and Kubo T., *New J. Phys.*, **9** (2007) 113.
[15] Loss D. and Sukhorukov E. V., *Phys. Rev. Lett.*, **84** (2000) 1035.
[16] Zhang G. B., Wang S. J. and Li L., *Phys. Rev. B*, **74** (2006) 085106.
[17] Dong B., Lei X. L. and Horing N. J. M., *Phys. Rev. B*, **77** (2008) 085309.
[18] Peng J., Wang B. and Xing D. Y., *Phys. Rev. B*, **71** (2005) 214523.
[19] Lu W., Ji Z., Pfeiffer L., West K. W. and Rimberg A. J., *Nature*, **423** (2003) 422.
[20] Fujisawa T., Hayashi T., Hirayama Y. and Cheong H. D., *Appl. Phys. Lett.*, **84** (2004) 2343.
[21] Gustavsson S. *et al.*, *Phys. Rev. Lett.*, **96** (2006) 076605.
[22] Sukhorukov E. V. *et al.*, *Nat. Phys.*, **3** (2007) 243.
[23] Fujisawa T., Hayashi T., Tomita R. and Hirayama Y., *Science*, **312** (2006) 1634.
[24] Welack S., Esposito M., Harbola U. and Mukamel S., *Phys. Rev. B*, **77** (2008) 195315.
[25] Brandes T., *Ann. Phys. (Berlin)*, **17** (2008) 477.
[26] Welack S., Maddox J. B., Esposito M., Harbola U. and Mukamel S., *Nano Lett.*, **8** (2008) 1137.
[27] Chang D. I. *et al.*, *Nat. Phys.*, **4** (2008) 205.
[28] Welack S., Schreiber M. and Kleinekathöfer U., *J. Chem. Phys.*, **124** (2006) 044712.